PRZEGLĄD ELEKTROTECHNICZNY

Ukazuje się od 1919 roku

12'19

Organ Stowarzyszenia Elektryków Polskich • **Wydawnictwo SIGMA-NOT Sp. z o.o.**

Invited paper

Jacek F. GIERAS

UTP University of Science and Technology, Bydgoszcz, Poland

doi:10.15199/48.2019.12.01

Design of high-speed permanent magnet machines

Abstract. *The actual trend in high speed electromechanical drives technology is to use permanent magnet (PM) brushless motors The following issues, which are essential in electromagnetic, mechanical and thermal design of high-speed PM brushless motors have been discussed: 1) main dimensions and sizing procedure, 2) mechanical requirements, 3) stator design guidelines including bad practices, 4) rotor design guidelines, 5) retaining sleeves (cans), 6) losses in the rotor, 7) thermal and cooling issues.*

Streszczenie. *We współczesnych napędach elektromechanicznych wysokiej prędkości stosowane są głównie silniki bezszczotkowe o magnesach trwałych. W artykule przedstawiono najważniejszcze problemy wystepujące w projektowaniu tych maszyn: 1) wymiary główne, 2) wymagania mechaniczne,3) projektowanie stojana z uwzględnieniem złych praktyk, 4) projektowanie wirnika, 5) tuleja nieferromagnetyczna wirnika, 6) straty w wirniku, 7) zagadnienia cieplne oraz chłodzenie - (**Projektowanie maszyn wysokoobrotowych o magnesach trwałych)***

Keywords: high speed electrical machines, permanent magnet, design, main dimensions, losses, requirements, retaining sleeve.
Słowa kluczowe: maszyny elektryczne wysokiej predkości, magnesy trwałe, wymiary główne, straty, wymagania, tuleja wirnika.

Introduction

High-speed permanent magnet (PM) machines that develop rotational speeds in excess of 5000 rpm are necessary for centrifugal and screw compressors, grinding machines, mixers, pumps, machine tools, textile machines, drills, handpieces, aerospace, microturbines, flywheel energy storages, turbochargers, etc [1,2,8,9]. The actual trend in high speed electromechanical drives technology is to use PM brushless motors, solid rotor induction motors or switched reluctance motors. The highest efficiency and highest power density is achieved with PM brushless motors. Design guidelines for high speed PM brushless motors include, but are not limited to [9]:

- Compact design, high power density and minimum number of components;
- High efficiency and power factor close to unity over the whole range of variable speed and variable load;
- Ability of the PM rotor to withstand high temperature (losses in retaining sleeve and PMs);

Active and passive materials used for the rotor should be thermally compatible, i.e., with similar coefficient of thermal expansion;

- SmCo PMs rather than NdFeB PMs should be used if the PM rotor is integrated with turbine rotor;
- Optimal cost-to-efficiency ratio to minimize the cost-to-output power ratio of the system;
- High reliability (failure rate < 5% within 80,000 h);
- Low cogging torque and vibration level;
- low total harmonics distortion (THD).

Main dimensions

Classical sizing procedure of electrical machines uses the so called "output equation" [4,7,11]. The output equation requires estimation of the magnetic flux density in the air gap (T) and stator line current density (A/m). Even for experienced designer, it is difficult to estimate the line current density for a given type of a high-speed machine. Much more convenient is to use the current density in stator conductors (A/mm^2) because the current density in conductors allows for estimation of the Joule's losses and selection of cooling system at the early stage of the design procedure. Given below is the alternative method of estimation of main dimensions of electrical machines, which is designer-friendly, especially for high-speed PM machines.

The electromagnetic apparent power S_{elm}, phase EMF E_f, and rotor magnetic flux Φ_f of an AC electrical machine are, respectively

$$S_{elm} = m_1 E_f I_a \tag{1}$$

$$E_f = \pi\sqrt{2}\, f\, N_1 k_{w1} \Phi_f \tag{2}$$

$$\Phi_f = \frac{2}{\pi} B_{mg} \tau L = \frac{1}{p} B_{mg} D_{1in} L \tag{3}$$

where m_1 is the number of stator (armature) phases, I_a is the *rms* armature current per phase, f is the frequency of the armature current, N_1 is the number of stator turns in series per phase, k_{w1} is the stator winding factor for the fundamental space harmonic, B_{mg} is the peak value of the normal component of the air gap magnetic flux density, $\tau = \pi D_{1in}/(2p)$ is the pole pitch, D_{1in} is the stator core inner diameter, L is the axial length of the stator ferromagnetic stack, and p is the number of pole pairs. Thus, the electromagnetic apparent (internal) power is

$$\begin{aligned} S_{elm} &= m_1 \pi\sqrt{2}\, f\, N_1 k_{w1} \frac{1}{p} B_{mg} D_{1in} L I_a \\ &= m_1 \pi\sqrt{2}\, n_s N_1 k_{w1} B_{mg} D_{1in} L I_a \\ &= m_1 \pi\sqrt{2}\, n_s N_1 k_{w1} B_{mg} D_{1in} L J_a s_a \end{aligned} \tag{4}$$

where the synchronous speed $n_s = f/p$, the stator (armature) current density $J_a = I_a / s_a$, and s_a is the cross section of bare conductors including parallel wires. Using the slot fill factor k_{fill} defined as the ratio of pure copper area ($2m_1N_1s_a$)–to–slot cross-section area A_{slot}, the slot area and slot-tooth zone area A_{sl} are, respectively

(5) $A_{slot} = \frac{2m_1 N_1 s_a}{k_{fill}} \qquad A_{sl} = \pi \frac{D_{1y}^2 - D_{1in}^2}{4} = \frac{\pi}{4} D_{1in}^2 (k_y^2 - 1)$

where D_{1y} is the inner diameter of the stator yoke (bottoms of slots) and the coefficient $k_y = D_{1y}/D_{1in}$ depends on the number of poles. Since the radial height of the stator yoke is inversely proportional to the number of poles, for most AC electrical machines.

(6) $$k_y = \frac{D_{1y}}{D_{1in}} \approx 1.05 + \frac{1}{1.5p}$$

Thus,

(7) $$S_{elm} = \frac{\pi^2}{6\sqrt{2}} n_s k_{w1} k_{fill} B_{mg} L J_a D_{1in}^3 (k_y - 1)$$

and, on the other hand,

(8) $$S_{elm} = m_1 E_f I_a = m_1 \varepsilon V_1 I_a = \frac{\varepsilon P_{out}}{\eta \cos\varphi}$$

where η is the efficiency, $\cos\varphi$ is the power factor, $\varepsilon = E_f / V_1$, V_1 is the phase voltage and the output power is $P_{out} = m_1 V_1 I_a \eta \cos\varphi$. Comparing right hand sides of the above equations (7) and (8)

(9) $$\frac{\varepsilon P_{out}}{\eta \cos\varphi} = \frac{\pi\sqrt{2}}{3} n_s k_{w1} k_{fill} B_{mg} J_a \left(\frac{\pi}{4} D_{1out}^2 L \right) D_{out} \frac{1}{k_D^3} (k_y - 1)$$

where the ratio of the outer–to–inner diameter of the stator

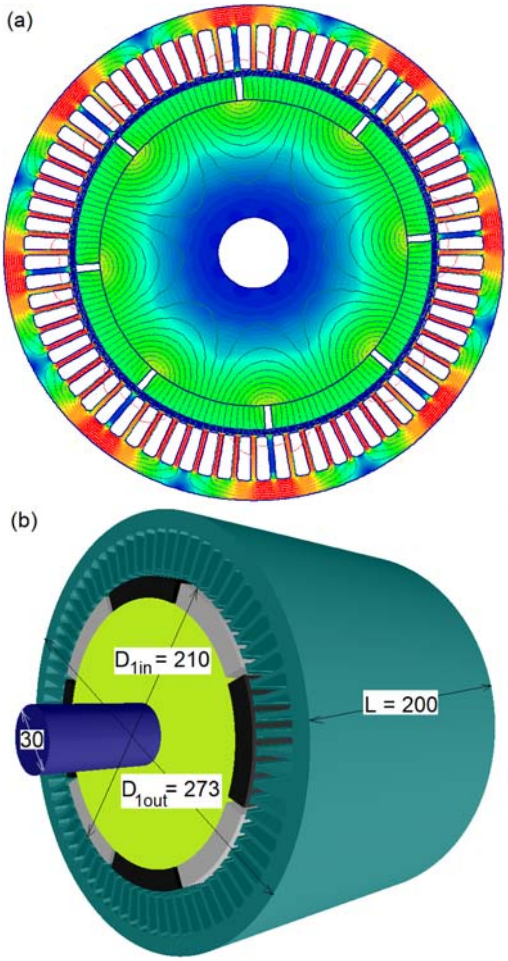

Fig. 1. High speed, 8-pole, 72-slot PM brushless generator rated at 1.5 MW, 15 krpm, 620 V: (a) cross section with 2D magnetic flux distribution; (b) main dimensions. The air gap including the thickness of retaining sleeve is 2.8 mm, radial thickness of SmCo SS3218 PMs is 13.6 mm (B_r = 1.155 T, H_c = 1259 kA/m), slot fill factor k_{fill} = 0.5, armature current = 1491 A, efficiency = 98% and power factor = 0.9465.

(10) $$k_D = \frac{D_{1out}}{D_{1in}} \qquad k_D \cong 1.75 \qquad \text{if} \quad p = 1$$

$$k_D \cong 1.05 + \frac{1}{p} \quad \text{if} \quad p < 1 \le 20$$

The volume of the active parts of the machine is $V = 0.25\pi D_{1out}^2 L$ and the VD_{1out} product

(11) $$VD_{1out} = \frac{3\varepsilon k_D^3 P_{out}}{\pi\sqrt{2}\, n_s k_{w1} k_{fill} (k_y^2 - 1) B_{mg} J_a}$$

Alternatively, the inner diameter D_{1in} of the machine can be found as

(12) $$D_{1in} = \sqrt[3]{\frac{6\sqrt{2}\varepsilon P_{out}}{\pi^2 k_{w1} k_{fill} \left(k_y^2 - 1\right) n_s L B_{mg} J_a \eta \cos\varphi}}$$

Examples of calculations of main dimensions on the basis of eqns (11) and (12) and their comparison with prototypes or calculations using another approach are shown in Table 1. This comparison confirms the accuracy of eqns (11) and (12). The machine rated at 1.5 MW and 15 krpm is a generator designed for directed energy weapon (DEW) systems (Fig. 1).

Table 1. Comparison of dimensions of prototypes with dimensions obtained from eqns (11) and (12).

Machine	How the results have been obtained	D_{1in}/D_{1out} mm	L, mm	Mass of active components, kg
92 kW, 41 krpm, J_a = 10.3 A/mm^2 4-pole motor	prototype	65/125.5	102.9	8.2
	eqns (11), (12)	78/125.5	93.5	7.4
48.5 kW, 43 krpm, J_a = 6.62 A/mm^2,4-pole motor	prototype	45/98.5	128.0	8.7
	eqns (11), (12)	46/98.0	126.0	8.2
1.5 MW, 15 krpm, J_a = 16.8 A/mm^2, 8-pole generator	SPEED *Adapco*	205.6/280	200	88.0
	eqns (11), (12)	210/273	200	88.7

Mechanical requirements

The rotor diameter is limited by the bursting stress at the design speed. The rotor axial length is limited by its *stiffness* and the *first critical* (whirling) speed. Since the centrifugal force acting on a rotating mass is proportional to the linear velocity square and inversely proportional to its radius of rotation, the rotor must be designed with a small diameter and must have a very high mechanical integrity. The surface linear speed (tip speed) of the rotor

(13) $$v = \pi \left(D_{1in} - 2g \right) n_s = \pi \left(D_{1in} - 2g \right) \frac{f}{p}$$

where g is the air gap (mechanical clearance). The maximum permissible surface linear speed depends on the rotor construction and materials.

When the shaft rotates, centrifugal force will cause it to bend out (Fig. 2). For a single rotating mass m the first critical (whirling) rotational speed and first critical angular speed are, respectively [4,10,12]

(14) $$n_{cr} = \frac{1}{2\pi} \sqrt{\frac{K}{m}} \qquad \Omega_{cr} = \sqrt{\frac{K}{m}}$$

The static deflection takes the form

$$\sigma = \frac{mgL_{sh}^3}{48EI} = \frac{mg}{K} \tag{15}$$

where the stiffness is

$$K = 48\frac{EI}{L_{sh}^3}, \tag{16}$$

the area moment of inertia $I = \pi D^4/64$, EI is the bending stiffness and L_{sh} is the bearing span (Fig. 2a). Distinguishing between the rotor stack (E, I, L_r) and shaft (E_{sh}, I_{sh}, L_{sh}), the stiffness of the shaft with rotor stack is [4,12]

$$K = 48\frac{EI}{L_r^3} + 48\frac{E_{sh}I_{sh}}{L_{sh}^3} \tag{17}$$

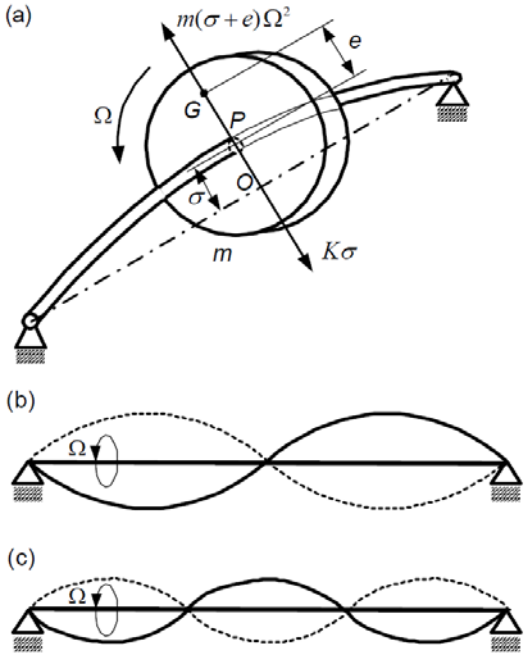

Fig. 2. Single mass flexible rotor with residual unbalance and possible modes of oscillations: (a) 1st mode; (b) 2nd mode; (c) 3rd mode. O – center of rotation, G – center of gravity, P – geometric center.

The modulus of elasticity of the laminated stack E is from 1 to 20% of the modulus of elasticity E_{sh} of the steel shaft. The stronger the clamping of laminations, the higher the modulus E.

Neglecting damping, the centrifugal force is $m(\sigma + e)\,\Omega^2$ and the restoring force (deflection force) is $K\sigma$, in which σ is the shaft deflection, e is imbalance distance (eccentricity) and $\sigma + e$ is the distance from the center of rotation to the center of gravity (Fig. 2). From the force balance equation [5,12]

$$K\sigma = m(\sigma + e)\Omega^2 \tag{18}$$

the deflection of the shaft can be found as

$$\sigma = \frac{m\Omega^2 e}{K(1 - m\Omega^2/K)^2} = \frac{e}{(\Omega_{cr}/\Omega)^2 - 1} \tag{19}$$

The shaft deflection $\sigma \to \infty$ if $\Omega = \Omega_{cr}$. No matter how small the imbalance distance e is, the shaft will whirl at the natural frequency. The mass rotates about the center of rotation O if $\Omega < \Omega_{cr}$ (Fig.2) Point O and G are opposite each other. The mass rotates about the center of gravity G if $\Omega > \Omega_{cr}$. Point O approaches point G.

It is recommended that the synchronous (rated) speed n_s of the machine should meet the following conditions [4]:

- if $n_s < n_{cr}$, when n_{cr} is the first critical speed of the rotor, then

$$n_s > 0.75\frac{n_{cr}}{2p} \quad \text{or} \quad n_s < 1.33\frac{n_{cr}}{2p} \tag{20}$$

- if $n_s > n_{cr}$, then

$$n_s > 1.33 n_{cr} \tag{21}$$

With the radial magnetic pull being included, the first critical speed is [4]

$$n_{cr} = \frac{1}{2\pi}\sqrt{\frac{K - K_e}{m}} \tag{22}$$

where K_e is the negative spring coefficient (stiffness) induced by the electromagnetic field (magnetic pull). This coefficient is given, e.g., in [4].

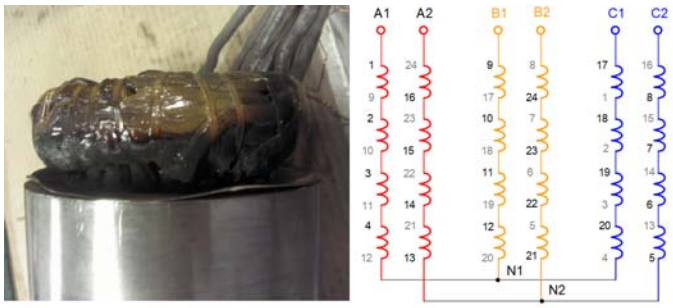

Fig. 3. Duplex winding. Unavoidable small phase shift between two systems of windings can arise high currents that can damage thermally the stator winding (damaged end turns are shown).

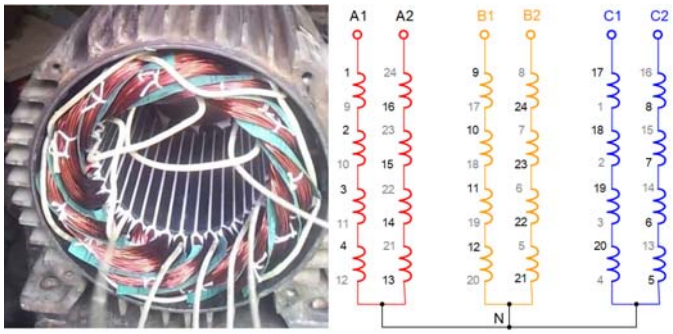

Fig. 4. Parallel paths can cause circulating currents in the auto-wound stator due to random positions of conductors in coils.

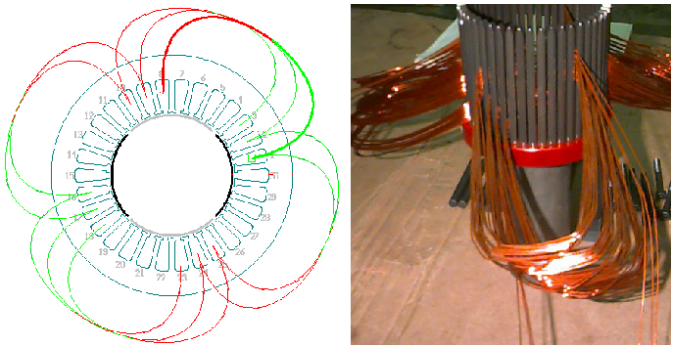

Fig. 5. Concentric double-layer winding with coil groups containing different number of coils is a wrong solution. Double-layer lap winding is recommended. It can be auto wound.

Electromagnetic design

Given below are the fundamental issues, which are essential in electromagnetic, mechanical and thermal design of high- speed PM brushless machines

[1,2,3,7,8,9,10,15]:

- Volume and mass: the higher the speed, the higher the power density;
- Power losses and efficiency: special attention must be given to windage and core losses;
- Laminations: cobalt alloy, non-oriented silicon steel or amorphous alloy laminations;
- Stator conductors: small diameter stranded conductors or Litz wires;
- Higher harmonics generated by the solid-state converters: their influence on losses, vibration and noise;
- Cooling system: intensive air or oil cooling system;
- Rotor tensile hoop stresses: properly selected rotor diameter, rotor diameter–to–length ratio and rotor retaining sleeve;
- Thermal compatibility of rotor materials to avoid compressing stresses on PMs that fluctuates with the temperature;
- Rotor dynamics: the first critical speed of the rotor should be much higher or much lower than the rated (synchronous) speed – eqns (20) and (21).

A. Stator design

The stator core is stacked of slotted or slotless laminations. For input frequencies 400 Hz and lower, 0.2 to 0.35-mm thick laminations are used. For higher frequencies, 0.1-mm laminations are necessary. Vacuum impregnated coils made of stranded conductors are inserted into slots. To minimize the space harmonics, the stator winding is made as a double layer winding with shorted coils. For very high speeds and low voltages, when the EMF induced in single turn stator coils is too high, small number of coils, single layer winding or parallel paths (not recommended) must be used. Hollow conductors and direct water cooling are too expensive for machines rated below 200 kW. The stator volume is affected by winding losses and heat dissipation.

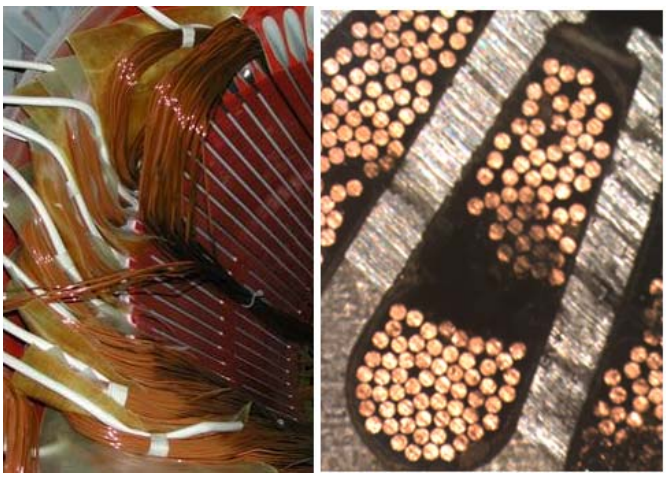

Fig. 6. Deep slots for auto wound double-layer windings with parallel paths are not recommended. Winding asymmetries due to coil side locations in the slot lead to unequal impedances and unequal induced EMFs.

In order to avoid circulating currents, excessive winding losses and hot spots in the stator winding, it is necessary to avoid:

- *Duplex windings* (Fig. 3). Duplex winding works well for induction machines, but it is not acceptable for high speed PM machines.
- *Parallel paths* (Fig. 4). There are circulating currents in parallel paths of the auto-wound stator due to random position of conductors in coils.
- *Concentric winding* (Fig. 5). Concentric double-layer winding with coil groups containing different number of coils is not recommended. It is much better to use double-layer lap winding instead. Double-layer lap winding can be auto wound.
- *Deep slots* (Fig. 6). Deep slots for auto wound double-layer windings with parallel paths are not recommended. Winding asymmetries due to coil side location in the slot, lead to unequal impedances and unequal induced EMFs. This causes circulating currents and more importantly, very uneven distribution of the currents within the strand conductors (parallel wires) of the same phase.

To minimize the losses in the retaining sleeve and PMs, torque ripple and vibration, the stator slots should have very narrow slot openings or be closed. In the case of closed stator slots, the slot closing bridge should be highly saturated under normal operating conditions.

B. Rotor design

PM rotor designs (Fig. 7) include surface-type, inset-type, bread loaf or interior-type PMs [7]. All surface-type PM rotors are characterized by minimal leakage flux. Bread loaf surface-type PM rotors provide, in addition, the highest magnetic flux density in the air gap (large volume of PM material).

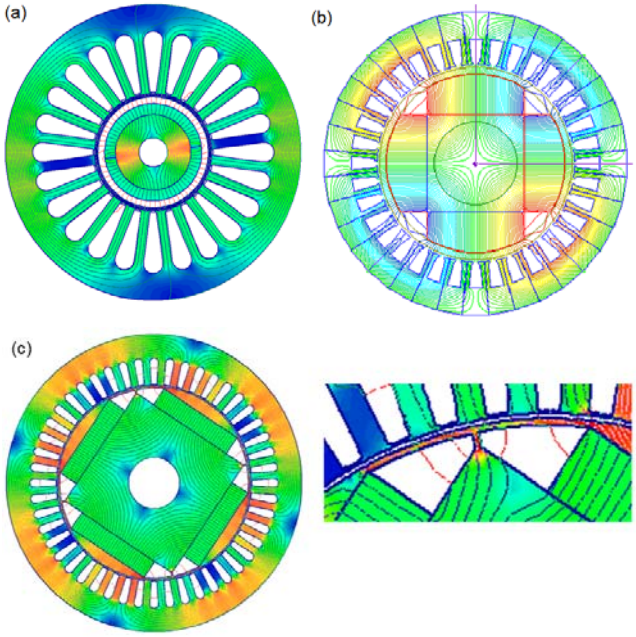

Fig. 7. High-speed PM rotor designs: (a) surface PM rotor provides minimal leakage flux); (b) bread-loaf surface-type PM rotor provides the highest magnetic flux density in the air gap (large volume of PM material); (c) interior-type PM rotor does not need any retaining sleeve, but the ferromagnetic bridge in the rotor core between neighboring PMs must be very carefully sized.

All surface-type, including bread loaf and inset-type PM rotors, can be used only with an external rotor retaining sleeve (can) [6]. In the case of an interior-type PM rotors the retaining sleeve is not necessary, but the ferromagnetic bridge in the rotor core between neighboring PMs (Fig. 7c) must be very carefully sized. From electromagnetic point of view, this bridge should be very narrow to obtain full saturation, preventing the circulation of leakage flux between neighboring rotor poles. From a mechanical point of view, this bridge cannot be too narrow to withstand high mechanical stresses. In practice, interior-type PM rotors without retaining sleeves can be used at speeds not exceeding 6000 rpm.

Good materials for retaining sleeves are nonferromagnetic and have high permissible stresses, low electric conductivity, low specific mass density and good thermal conductivity. Typical materials for nonferromagnetic sleeves are Inconel 718 (NiCoCr based alloy) with electric conductivity 0.8×10^6 S/m (1.38% ICACS) at 20°C, titanium alloys, stainless steels, carbon graphite, carbon fiber, glass fiber and reinforced plastics.

Fig. 8. Retaining sleeves for high speed PM rotors: (a) metal sleeve; (b) carbon-graphite sleeve.

Fig. 9. Rotor of a 100 kW, 70 krpm PM brushless motor for an oil free compressor. 1 – PM rotor with retaining sleeve, 2 – foil bearing journal sleeve. Photo courtesy of Mohawk Innovative Technology, Albany, NY, USA.

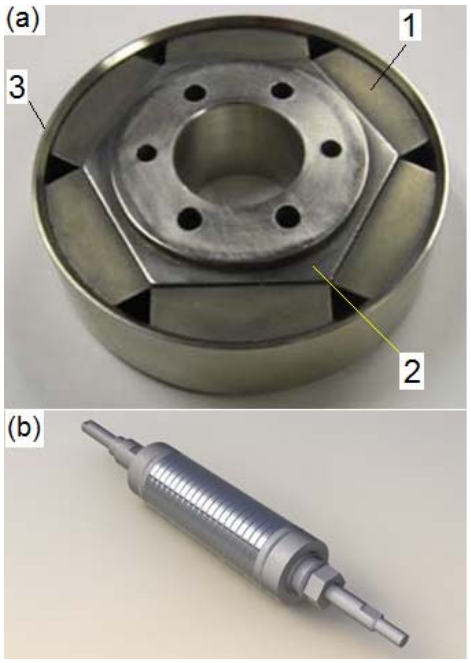

Fig. 10. PM rotor of segmented construction of a six-pole high speed PM brushless motor with metal retaining sleeve: (a) single segment; (b) rotor stacked with 20 segments. 1 — PM, 2 — rotor core, 3 — retaining sleeve (can). Photo courtesy of Electron Energy Corporation, Landisville, PA, USA.

Maximum temperature for metal sleeves (Fig. 8a) is 290°C and for fiber sleeves (Fig. 8b) is 180°C. Maximum surface linear speed for metal sleeves is 240 m/s and for fiber sleeves is 320 m/s. There are practically no eddy-current losses in fiber sleeves; however, it is more difficult to assembly the rotors with fiber sleeves than rotors with metal sleeves. If the magnetic saturation effect is used effectively, a thin steel sleeve in low power machines can sometimes be better than a sleeve made of nonferromagnetic material.

The allowable stress on the PMs is 80 N/mm^2. To prevent the magnets from exfoliating, initially, a nonferromagnetic stainless steel sleeve is shrunk on the PMs to retain them. Although the stainless steel has low electric conductivity, the losses occurred in a relatively thick sleeve can be still quite large at the speeds over 100,000 rpm. Nonconductive fiber reinforced plastic at higher speeds is better.

A good manufacturing practice is to use segmented rotors, which allows for using the same segment (module) for different ratings of machines and leads to reduction of cost of fabrication. A six-pole rotor segment is shown in Fig. 10a. The PMs are of bread loaf type and are contained with the rotor hub in a nonferromagnetic metal can. The number of rotor segments depends on the machine rating (Fig. 10b).

To increase the electromagnetic coupling between the magnets and the stator winding, the air gap should be made as small as mechanically possible. However, the use of a small air gap increases the tooth ripple losses in the retaining sleeve, if the sleeve is made of current-conducting material.

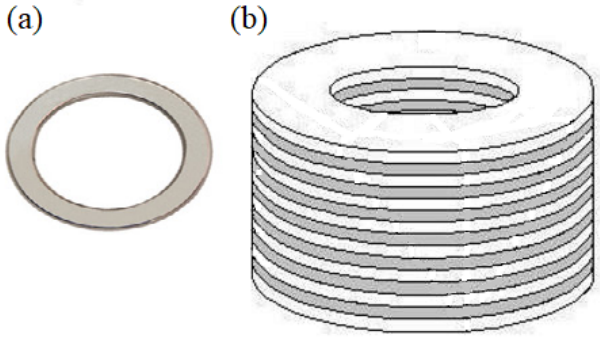

Fig. 11. Laminated retaining sleeve: (a) single non-ferromagnetic lamination; (b) stacked retaining sleeve.

Recently, laminated sleeves stacked from non-ferromagnetic materials have been investigated [15,16]. They provide:

- significant reduction of eddy currents;
- simple manufacture using punching dies;
- can withstand high radial stresses.

The disadvantage is the limit on the radial thickness of the laminated sleeve: the sleeve cannot be too thin.

Active radial and axial magnetic bearings or air bearings are frequently used. High-speed PM brushless motors integrated with magnetic bearings and solid-state devices are used in gas compressors providing a true oil free system, reduced maintenance and high efficiency. No auxiliary lubrication supply system is needed, eliminating hazardous waste disposal issues.

Rotor losses

In PM synchronous and PM DC brushless motors the rotor core losses due to fundamental harmonic do not exist. The rotor core losses in PM brushless machines are due to the pulsating flux produced by the rapid changes in the air gap reluctance as the rotor passes the stator teeth. These losses are negligible in surface-mounted PM motors, due to their large effective air gaps (including PM radial thickness).

These rotor losses can sometimes be significant in buried PM motors, salient pole rotors and surface PM motors with mild steel pole shoes. The rotor core losses due to magnetic flux pulsations and higher harmonics can be calculated using, e.g., methods described in [6,7,11,13].

A. Losses in conductive retaining sleeves

The slot ripple losses in the retaining sleeve of the rotor can be calculated with the aid of the following simple analytical equation [6,13]

$$\Delta P_{sl} = \frac{\pi^3}{2}\sigma_{sl} k_r (B_{msl} n)^2 D_{sl}^3 l_{sl} d_{sl} \text{ [W]} \quad (23)$$

where n is the rotor speed in rev/s, $D_{sl} = D_{2out} - d_{sl}$, D_{2out} is the rotor outer diameter, D_{sl}, l_{sl}, d_{sl} and σ_{sl} are the mid-diameter in meters, effective length in meters, thickness in meters and the electric conductivity in S/m of the retaining sleeve, respectively. For titanium alloy IMI250 the electric conductivity σ_{sl} = 0:625 × 10^6 S/m at 20^{0}C. The coefficient for increasing the sleeve resistance due to tangential sleeve currents is [7]

$$k_r \approx 1 + \frac{1}{\pi}\frac{t_1}{l_{sl}} \quad (24)$$

The amplitude of the high frequency magnetic flux density due to slot openings (slot ripple) can be calculated according to Richter [11]

$$B_{msl} = 2\beta B_{mean} = 2\beta \frac{1}{k_C}\frac{2}{\pi} B_{mg} \quad (25)$$

where

$$\beta = \frac{B_{msl}}{2B_{mean}} = \frac{1+u^2-2u}{2(1+u^2)} \quad (26)$$

$$u = \frac{b_0}{2g} + \sqrt{1+\left(\frac{b_0}{2g}\right)^2} \quad (27)$$

and B_{mean} is the mean value of the magnetic flux density in the air gap under the stator slot opening, B_{mg} is the peak value of the magnetic flux density in the air gap, b_0 is the stator slot opening in m, g is the air gap between the stator core and PM, and k_C is Carter's coefficient of the air gap. Decrease in the slot opening and/or increase in the air gap reduce the slot ripple. For example, for an *Inconel* 718 sleeve with its electric conductivity σ_{sl} = 0:5295 × 10^6 S/m at 100^{0}C, diameter D_{sl} = 0.1 m, length l_{sl} = 0.1 m, and thickness d_{sl} = 1.6 mm the slot ripple losses in the sleeve are ΔP_{sl} = 1411 W at n = 100,000 rpm, ΔP_{sl} = 353 W at n = 50,000 rpm and ΔP_{sl} = 14 W at n = 10,000 rpm. The following machine parameters have been assumed: number of pole pairs p = 2, number of slots s_1 = 36, b_0 = 2 mm, g = 3.2 mm, B_{mg} = 0.7 T, which give u = 1.36 and B_{msl} = 0.02 T. Losses in the sleeve due to other harmonics can also be calculated with the aid of eqn (21) putting instead of B_{msl} the amplitude of the considered higher harmonic.

B. Losses in permanent magnets

The electric conductivity of sintered NdFeB magnets is from 0.6 to 0.85 × 10^6 S/m. The electric conductivity of SmCo magnets is from 1.1 to 1.4 × 10^6 S/m. Since the electric conductivity of rare earth PMs is only 40 to 96 times lower than that of a copper conductor, the losses in conductive PMs due to higher harmonic magnetic fields produced by the stator cannot be neglected in the case of high-speed motors.

Similar to losses in a conductive retaining sleeve, the most important losses in PMs are those generated by the fundamental frequency magnetic flux due to the stator slot openings. Slot ripple losses are only in motors with slotted armature ferromagnetic cores and do not exists in slotless machines.

The slot ripple losses in PMs can be approximately estimated using eqn (23), in which $\sigma_{sl} = \sigma_{PM}$, $l_{sl} = l_M$, $D_{sl} = D_{2out} - h_M$ and $d_{sl} = h_M$, where σ_{PM} is the electric conductivity of PM, l_M is the axial length of PM (usually $l_M = L_r$) and h_M is the radial height of PM, i.e.,

$$\Delta P_{PM} = \frac{\pi^3}{2}\sigma_{PM} k_r (B_{msl} n)^2 \left(D_{2out} - h_M\right)^3 l_M h_M \text{ [W]} \quad (28)$$

Since the external surface area of PMs is smaller than that of the rotor, eqn (23) should be multiplied by the factor $S_{PM}/(\pi D_{2out} l_M)$, where S_{PM} is the surface area of PMs. For surface PMs

$$S_{PM} = \alpha_i \pi D_{2out} L_r \quad (29)$$

The magnetic flux density B_{msl} can be estimated on the basis of eqn (25) only if the rotor is not equipped with conductive retaining sleeve. Otherwise, the realistic peak value B_{msl} will be much smaller. Eqn (25) may give in this case too high value of slot ripple losses in PMs. Power losses in PMs due to the νth higher space harmonic can be estimated on the basis of the 2D electromagnetic field distribution [7].

Rotor losses

Table 2 contains typical current densities for high-speed electrical machines with different cooling systems.

Table 2. Typical current densities for electrical machines with different cooling systems.

Cooling system	Current density [A/mm^2]
Totally enclosed machine, natural ventilation	4.5 to 6.0
Fins or heat sinks, natural ventilation	6.0 to 10.0
Totally enclosed machine, external blower	7.0 to 11.0
Through-cooled machine, external blower	14.0 to 15.0
Water or oil jacket	12.0 to 15.5
Spray oil-cooled end turns of stator and/or rotor	23.0 to 28.00
Direct cooling and hollow conductors	up to 30.0

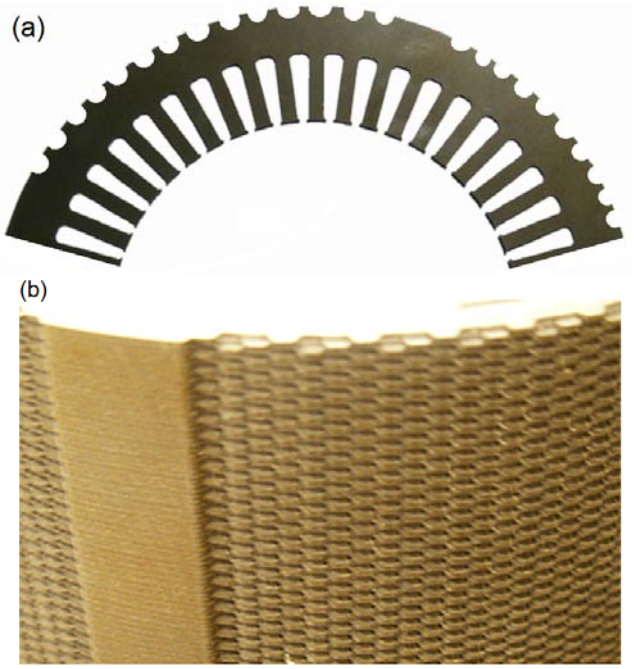

Fig. 12. Stator yoke (back iron) with serrated external surface: (a) single lamination; (b) stator stack. Neighboring laminations are shifted one from each other by half of the fin pitch.

The stator yoke (back iron) with serrated external surface behaves similar like a surface with fins. Small fins are stamped in each lamination (Fig. 12a). The stator stack has neighboring laminations shifted one from each other by half of the fin pitch (Fig.12b). In this simple way, using natural cooling system, the current density in the stator winding can be increased from about 6 A/mm^2 (smooth external surface) to 10 A/mm^2.

Liquid cooling jackets may have circumferential tubing or axial tubing system (Fig. 13). Circumferential tubing system (Fig. 13a) is more difficult to manufacture, but there is more uniform cooling of external surface of the stack and hot spots can be avoided. Axial tubing system (Fig. 13b) is easier to manufacture, but there is less uniform cooling of external surface of the stack and probability of hot spots.

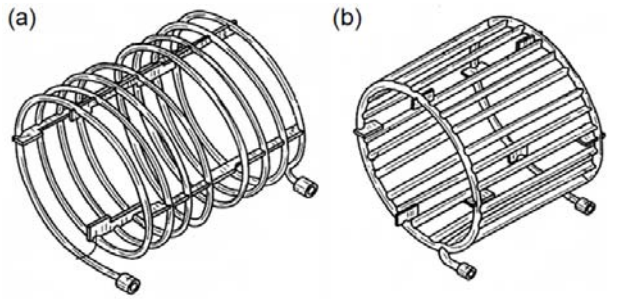

Fig. 13. Liquid cooling jackets: (a) circumferential tubing; (b) axial tubing.

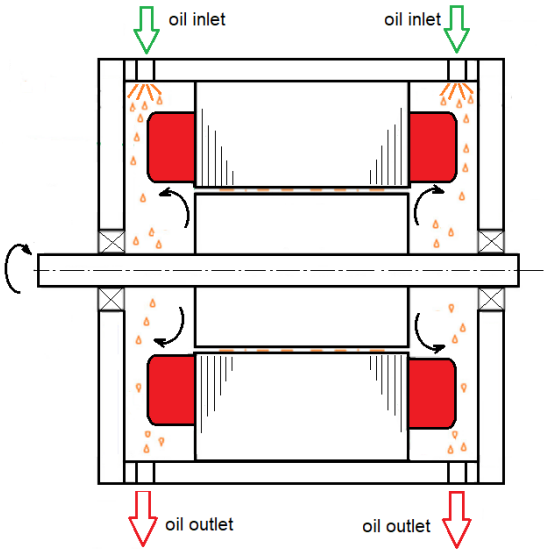

Fig. 14. Wet machine with spray-oil cooled end windings. Spray nozzles are installed in oil inlets.

Oil spray cooling system can be as effective as direct liquid cooling with hollow conductors (Fig. 14). The current density can achieve 28 A/mm^2. The oil is injected through the nozzles to the interior of the machine and cools directly the end turns. A liquid spraying process can be described as consisting of two phases: (a) breaking of the liquid into separate droplets, and (b) directing the liquid drops onto a surface of an object. Nozzles are usually made of brass and provide conical or flat spray distribution pattern.

The cooling can be even more intensive if the oil flow passages are created between conductors in slots. Such a cooling method is limited only to the stator windings. In the case of round conductors, oil passages are naturally created between conductors with cylindrical cross section (Fig. 15a). In the case of rectangular conductors, oil flow passages are formed using a removable “spacer” casting process during impregnation (Fig. 15b). Void (about 0.5 mm gap) is left by melting out wax or pulling out Teflon strip after resistance heat auto dispense (RHAD) gels/cures. The reminder of the slot is impregnated.

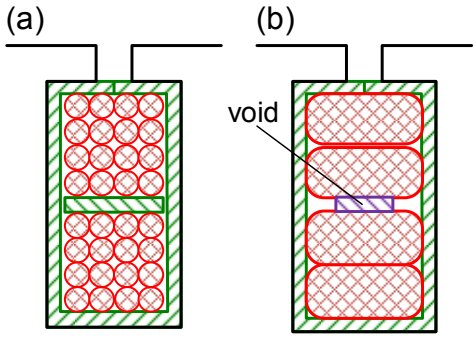

Fig. 15. Cross section of stator slots with double-layer windings: (a) coils wound with round conductors; (b) stiff coils made of rectangular conductors.

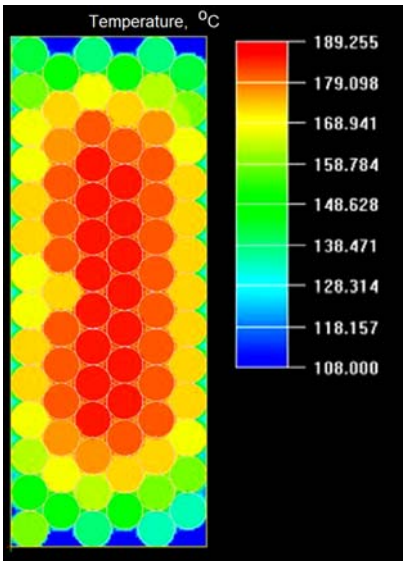

Fig. 16. Temperature distribution near stack edge at downstream end in the cross-section area of a rectangular slot with round conductors and oil flow through passages between conductors.

The temperature distribution in the cross-section area of a rectangular slot with round conductors and oil flow through passages between conductors is shown in Fig. 16.

Normally, conductors with insulation class F (180°C), 220°C or 240°C are used for stator windings. Nickel clad copper conductors with ceramic insulation can withstand higher temperatures, up to 600°C. DuPont™ Kapton® HN general purpose insulation films can be applied at temperatures up to 400°C.

Closing remarks

If the cost is not the primary issue, the objective function in the design of high-speed PM brushless machines is generally the maximum power density at given speed and cooling system. The power is limited by the thermal and mechanical constraints. The following aspects should be also considered [1,2,3,8,10,14,15,17,18]:

(a) *Mechanical design constraints* are important due to the high cyclic stress placed on the rotor components. Materials with high fatigue life are favored. Materials with low melting points, such as aluminum, should be avoided or restricted.

(b) *Dynamic analysis* of the rotor assembly, including shaft, core stack and bearing sleeves should be carried out with great detail using the 3D FEM simulation.

(c) *Static and dynamic unbalance.* Even a very small unbalance can produce high vibration. For example, a static unbalance of 0.05 N at a speed of 100,000 rpm produces an additional centrifugal force of more than 600 N.

(d) *Capital and operational costs* are generally directly linked. The use of magnetic bearings over traditional rolling element bearings or oil lubricated bearings is a very important consideration. The capital cost of magnetic bearings is high, but the operational costs are less since the rotational loss and power consumption are reduced and there is no maintenance.

Unbalance occurs when the center of gravity of a rotating object is not aligned with its center of rotation. Static unbalance is where the rotor mass center (principal inertia axis) is displaced parallel to the rotor geometric spin axis. Dynamic unbalance is where the rotor mass center is not coincidental with the rotational axis.

It is generally not difficult to design a high-speed PM brushless motor rated at a few kWs and speed 7000 to 20,000 rpm with efficiency about 93 to 95%. The efficiency of high-speed PM brushless motors rated above 80 kW and 70,000 to 90,000 rpm should be over 96%. Core losses, windage losses and metal sleeve losses are high. Slotless stator, amorphous cores and foil bearings can increase the efficiency up to 98%. High speed machines in multimegawatt range with slotted stator should also have efficiency close to 98%.

It is necessary also to mention, that intensive cooling system reduces only the volume envelope and mass of active components. As the cooling system becomes more effective, the current density in the stator winding increases and the winding losses (Joule's losses) increase too. So that the efficiency usually decreases, not increases. To keep very high efficiency, sometimes the machine must be oversized.

Closing remarks

1) PM brushless machines are the highest power density and highest efficiency standard electrical machines with the best dynamic performance;

2) The development of high-speed PM machine technology is stimulated by a need for increase in the power density, reliability, fault tolerance, new control strategies, more efficient cooling technologies, and other technical challenges [1,2,8,9,10,14,15,17,18];

3) The proposed new sizing equation (Section „Main dimensions") allows for easy estimation of main dimensions including selection of the stator cooling system at the early stage of design of a high-speed PM machine;

4) When designing the stator winding of a high-speed PM machine it is necessary to avoid: (a) duplex winding; (b) parallel paths; (c) concentric winding with different coil groups; (d) deep slots;

5) All surface-type, including bread-loaf and inset-type PM rotors, can be used only with an external retaining nonferromagnetic sleeve;

6) High speed PM brushless machines can reach power density up to 7.0 kW/kg (with liquid cooling) and efficiency 98% [6];

7) The predominant losses in high speed PM machines are core losses, windage losses and losses in the rotor retaining sleeve (if made of current-conducting material) [1,2,3,5,8,14,15,17];

8) While using intensive cooling system, increase in the current density usually reduces the efficiency of the machine; however, the volume envelope and mass of active components is reduced;

9) Oversizing the high-speed machine can be sometimes a good method to keep the efficiency at maximum level.

***Authors**: prof. dr hab. inż. Jacek F. Gieras, Life Fellow of IEEE, Uniwersytet Technologiczno-Przyrodniczy, Instytut Inzynierii Elektrycznej, Al. S. Kaliskiego 7, 85-796 Bydgoszcz, Poland. E-mail: jacek. gieras@utp.edu.pl*

REFERENCES

[1] Arkkio A., Jokinen T., Induction and permanent magnet synchronous machines for high-speed applications, *in Proc. ICEMS'15*, Nanjing, China, 2015, 871-876.

[2] Boglietti, A., Pastorelli, M., Profumo, F., High speed brushless motors for spindle drives, *in Proc. Int Conf on Synchronous Machines SM100*, vol 3, Zurich, Switzerland, 1991, 817–822.

[3] Cho, H.W., Yoon, A., Renner, N.J., Haran, K.S., Detailed electromagnetic analysis of a high specific power slotless permanent magnet motor with imbalanced armature windings, *in Proc. COMPUMAG'17*, Daejon, Korea, 2017, paper PB-M4-8.

[4] Dabrowski, M., *Construction of Electrical Machines*, in Polish, Warsaw, Poland: WNT, 1977.

[5] Dunkerley, S., On the whirling and vibration of shafts, *Proc. of the Royal Soc. of London*, vol. 54, 1893, 365–370.

[6] Gieras, J.F., Koenig, A.C., Vanek, L.D., Calculation of eddy current losses in conductive sleeves of synchronous machines, *in Proc. Int Conf on El. Machines ICEM'08*, Vilamoura, Portugal, paper ID 1061, 1998.

[7] Gieras, J.F., High-speed motors, in *Permanent Magnet Motor Technology: Design and Applications*, 3rd ed. Boca Raton, FL, USA: CRC Taylor & Francis, chapter 9, 2010, 403-445.

[8] Gieras, J.F., Design of Permanent Magnet Brushless Motors for high Speed Applications, Invited Keynote Speech No 2, *ICEMS'14*, Hanghzou, China, 2014.

[9] Gieras, J.F., Woo, B.C., Kang, D.H., Selected aspects of design of high-speed permanent magnet brushless machines, *in Proc. ICEMS 2018*, Jeju Island, Korea, 2018, S2-0186, 943-948.

[10] Kawashima, K., Shimada, A., Spindle motors for machine tools. Mitsubishi, *Electric Advance*, September 2003, 17-19.

[11] Richter, R., *Elektrische Machinen*, Band I, 3 Auflage, Basel, Switzerland: Birkhauser Verlag, 1967.

[12] Rao, J.S., *Rotor Dynamics*, 3rd ed. New Delhi, India: New Age Int. Publishers, 1983.

[13] Robinson, R.C., Rowe, I., Donelan, L.E., The calculations of can losses in canned motors, *AIEE Trans. PAS, Part III*, June 1957, 312–315.

[14] Saari J., Arkkio, A., Losses in high speed asynchronous motors, *in Proc. Int. Conf. on Elec. Machines ICEM'94*, vol 3, Paris, France, 1994, 704–708.

[15] Shen, J.X., High-speed permanent magnet AC machines and vehicle applications, Keynote Speech, *in Proc. ICEMS 2018*, Jeju Island, Korea, 2018.

[16] Han, T., Wang, Y.C., Qin, X.F., Shen, J.X., Investigation of various rotor retaining sleeve structures in high-speed PM brushless motors, *in Proc. ICEMS 2018*, Jeju Island, Korea, 2018, I1-1320, 109-114.

[17] Takahashi, T., Koganezawa, T., Su, G., Ohyama, K., A super high-speed PM motor drive system by a quasi-current source inverter*, IEEE Trans. on Industry Applications*, vol. 30, issue 3, March 1994, 683–690.

[18] Tenconi, A., Vaschetto, S., Vigliani, A., Electrical machines for high-speed applications: Design considerations and tradeoffs, *IEEE Transactions on Industrial Electronics*, vol. 61, issue 6, June 2014, 3022–3029.